Extrinsic self-trapping and negative U in semiconductors: A metastable center in InP

Michael Stavola, Mark Levinson, J. L. Benton, and L. C. Kimerling
AT&T Bell Laboratories, Murray Hill, New Jersey 07974
(Received 9 March 1984)

A fascinating electron-irradiation-induced defect (the M center) in n-type InP has been reported recently. Two entirely different capacitance transient spectra can be obtained for this center in the same sample (a p-n junction diode) depending upon its bias condition during the cool down to the initial measurement temperature ($\sim$30 K). We present a conceptually simple configuration-coordinate model that explains the unusual properties of this center. In our model the metastable center can exist in either of two configurations, one which displays a very large lattice relaxation, and another ordinary (no anomalously large lattice relaxation) configuration. Photoionization rates have been measured for the defect levels of the two different defect configurations as a function of photon energy. These data are used to confirm the qualitative properties of our model and to determine its parameters. Classification of the M-center behavior within the general context of self-trapped configurations is proposed.

I. INTRODUCTION

In electron-irradiated, n-type InP a defect[1-3] has recently been discovered by capacitance spectroscopy (the M center after Levinson *et al.*[2]) with fascinating metastable characteristics. Two entirely different defect spectra (each with a ladder of electronic levels) are observed for this center depending upon the electronic, thermal, and optical history of the system. In the original work on this center the multiple electron states that were observed led to the suggestion of an electrostatically driven, pairing-depairing reaction that gave rise to two different charge-state-dependent configurations of the defect.[1]

In this work a configuration-coordinate (CC) description[4] is constructed to explain the spectroscopic data relating to the M center and its configurational transformation. We find that the M center displays both self-trapping and negative-U characteristics, and that these phenomena are interrelated in so far as the same large lattice relaxation is responsible for each. Our CC model explains the essential physics of the M center's configurational transformation and is independent of the specific nature of the interaction and local distortion. An advantage of the CC approach is that it reduces a complicated system of electronic levels to a schematic diagram and, thus, simplifies the understanding of the systematics of the experimental data. Further, a CC diagram is constrained by the intimate connection between the thermally and optically induced transitions of the center, thereby allowing the internal consistency of the proposed scheme to be checked.

Describing the M center with CC diagrams places it in the general context of large lattice relaxation phenomena that have been observed for crystalline defects in recent years.[5,6] The work by Lang and Logan[7] on DX centers introduced self-trapping as a phenomenon that can be important for defects in semiconductor materials. The negative-effective-U concept has been applied to defects in crystalline solids to explain the behavior of the Si vacancy and B interstitial in Si.[8-12] In recent theoretical work general classifications of such defects have been developed.[13,14] Recombination-enhanced defect reactions are a class of lattice relaxation phenomena that are also closely related to the effects to be described in this paper.[15-17] Our description of the M center's novel properties provides new insights into large lattice relaxation phenomena.

This paper is organized as follows. In Sec. II the relevant capacitance spectroscopic data on the M center and its configurational metastability are reviewed. In Sec. III we present new optical data that provide insight into the nature of the M-center transitions. Section IV contains a description of a CC model constructed from the spectroscopic data on charge-state transitions and configurational relaxations. Section V contains a discussion of the extrinsic self-trapping phenomena displayed by the M center and other defects [DX (Refs. 7 and 18) centers, EL2 (Ref. 19), CdF_2:In (Refs. 6 and 20)] in a more general context. Section VI contains our concluding remarks.

II. REVIEW OF CAPACITANCE SPECTROSCOPY FOR THE M CENTER

We summarize the results obtained in previous capacitance spectroscopic studies [primarily deep-level transient spectroscopy (DLTS) and thermally stimulated capacitance (TSCAP)] that were undertaken to elucidate the properties of the M center.[1-3] The M center is a defect that is observed in 1-MeV electron-irradiated, undoped, nominally n-type liquid-encapsulated Czochralski-grown InP.

The DLTS spectra observed in p^+-n junctions or Schottky barrier diodes that characterize the *two different configurations* of the M center are shown in Fig. 1. The spectrum labeled configuration A is obtained if the specimen is cooled to the initial measurement temperature in darkness without an applied bias. Peak $A1$ has an electron-emission activation energy of 0.15 eV and an electron-capture cross section of 9×10^{-18} cm^2. The spec-

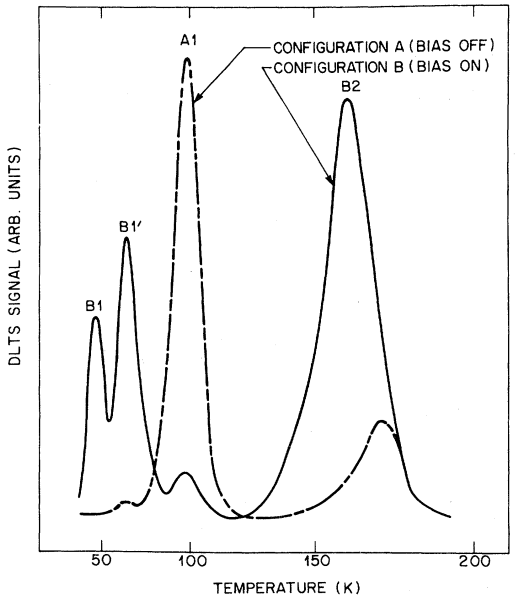

FIG. 1. DLTS spectra of the two M-center configurations.

trum labeled configuration B is obtained if the specimen is cooled with reverse bias applied. Peaks $B1$, $B1'$, and $B2$ have emission activation energies of 0.09, 0.14, and 0.37 eV, respectively.[21] The electron-capture cross sections were greater than 2×10^{-16} cm^2 for the three observed levels of configuration B.

Here we adopt a different notation than has been used in the earlier work on the M center in order to emphasize the multielectron physics of the center rather than the displacement damage defect-state spectrum.[1-3] We call the two different configurations of the defect A and B as is consistent with previous work. The emission features associated with configuration A are labeled $A1$, $A2$, and $A3$. The emission features associated with configuration B are labeled $B1$, $B1'$, and $B2$. Thus those features associated with each configuration are clearly labeled as such.

The three capacitance versus temperature (TSCAP) curves in Fig. 2 show the changes in charge contained in the diode depletion layer for the two configurations. The curves correspond to the following cases.

(a) Configuration A is obtained at the outset of the measurement by cooling at zero bias to 33 K. Reverse bias is then applied for the TSCAP rewarming procedure. The emission corresponding to DLTS peak $A1$ is seen. In addition, at higher temperature, the further emission of two electrons, $A2$ and $A3$, occurs together with the transformation from configuration A to B. (That is, if the specimen is cooled with reverse bias applied immediately following the emission of these two electrons, a DLTS spectrum shows that the M center is in configuration B.)

(b) Configuration B is obtained at the outset of the measurement by cooling to 33 K under applied reverse bias. The diode is shorted to zero bias to allow trap filling, and then warmed under reverse bias for the TSCAP measurement. Electron emissions corresponding to peaks $B1$, $B1'$, and $B2$ are seen.

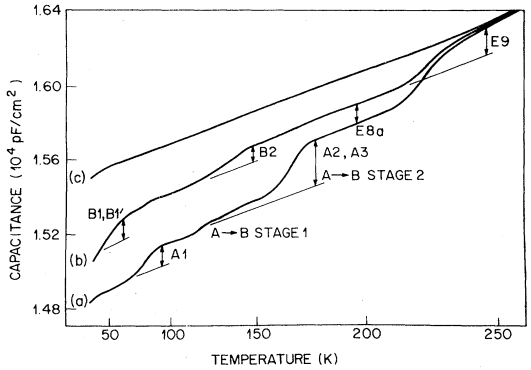

FIG. 2. TSCAP spectra of (a) configuration A, (b) configuration B, and (c) a reference.

(c) Curve C is a reference curve obtained by cooling with applied reverse bias and rewarming to obtain the temperature-dependent capacitance of the sample in configuration B without carrier emission.

The thermally activated transformation kinetics between configurations A and B have also been studied in detail.[1,3] The transformation $A\rightarrow B$ occurs (at 170 K in Fig. 2) with the simultaneous electron emissions $A2$ and $A3$. The transformation rate has been measured to be $k(A\rightarrow B)=10^{11}\exp[(-0.42\text{ eV}/kT]$. The $A\rightarrow B$ transformation actually has a complicated two-stage nature that is not presently understood. For the purposes of this publication the predominant $A\rightarrow B$ transformation process (stage 2 in Fig. 2) is emphasized. The transformation $B\rightarrow A$ occurs in the absence of bias with the rate $k(B\rightarrow A)=10^{7}\exp[(-0.24\text{ eV}/kT]$. This process has been interpreted as involving thermally activated electron capture which is consistent with the observed prefactor.

In Fig. 2 the emissions $E8a$ and $E9$ are due to other defects[21] that complicate the TSCAP. They have no bearing on the discussion of the M center here but account for the residual charge stored in the junction above the $A\rightarrow B$ transformation temperature in the TSCAP data.

III. PHOTOIONIZATION EXPERIMENTS FOR THE M CENTER

Our principal goal in this paper is to develop a CC model that will incorporate the various M-center charge-state transitions and configurational relaxations in a consistent fashion. New photoionization results are introduced to provide complementary information to the previous work on thermally activated transitions and to give insight into the nature of the transitions.

The following results from the previous study[2] have bearing on the forthcoming discussion. The transformation from configuration $A\rightarrow B$ occurs with optical excitation above a threshold photon energy of 0.8 eV at 101.6 K. There was no optically excited transformation from configuration $B\rightarrow A$ observed. The interpretation of these results was that electron emissions $A2$ and $A3$ could be excited optically and that emission $A3$ controlled the $A\rightarrow B$ transformation process. We shall now present

photoionization data specific to *each* charge state of the M center.

The defect charge states in our samples (p^+n mesa diodes) were monitored by measurement of the depletion-region capacitance with a Boonton model 72B capacitance meter. The sample was mounted on the cold finger of a variable temperature Dewar with an optical window. Both the TSCAP and photoionization experiments were performed with the same instrumentation. Variable-wavelength sample illumination was achieved with either a conventional tungsten lamp and grating monochromator or, when higher intensities were required, a Burleigh Instruments FCL-10 tunable color center laser. It was necessary to carefully eliminate sources of stray light because the M-center configuration is very sensitive to above-band-gap illumination (the transformation $A \rightarrow B$ occurs with the capture of photogenerated holes).[2] The mesa diodes were illuminated from the side.

To determine which photoionization processes occur for a given photon energy the following procedure was used. The sample was first cooled under the appropriate bias condition to obtain the desired M-center configuration, A or B. Then the diode was shorted to fill the traps at low temperature and a reverse bias was applied. The sample was illuminated with monochromatic light of given energy at low temperature. The charge state of the M center following illumination was then determined by measuring the capacitance versus temperature (TSCAP) spectrum. Sets of such spectra for configurations A and B are shown in Fig. 3. Once such measurements have been made as a function of photon energy to map out the photoionization thresholds of the various electronic emission processes, it is straightforward to set the defect in any desired charge state and to make further measurements on specific emission processes separately.

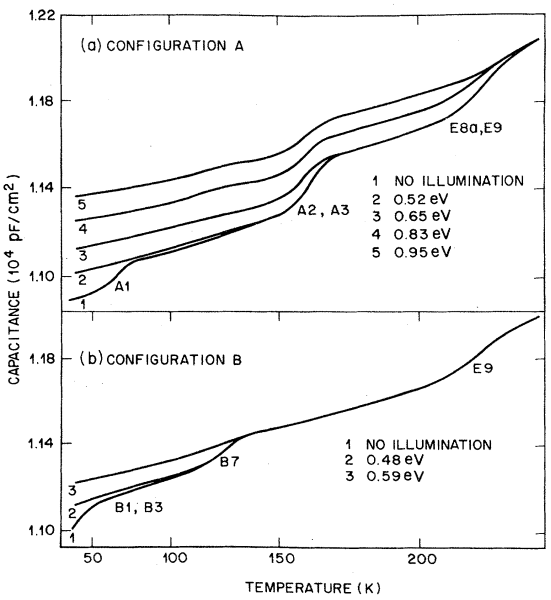

FIG. 3. TSCAP spectra taken following illumination at the indicated photon energy. The optical fluence (intensity times time of illumination) is constant for the different spectra.

Consistent with previous work,[2] the photoionization of configuration-B defect levels does not lead to configurational transformation. We find for configuration A that photostimulation of electron emission $A1$ and $A2$ [incident photon energies that lead to curves 3 or 4 in Fig. 3(a)] does not change the defect configuration. That is, following photostimulation of these emissions, if the defect levels are refilled by removing the reverse bias momentarily at low temperature, a TSCAP spectrum shows that the defect remains in configuration A. However, after electron emission $A3$ occurs, refilling the trap levels at low temperature and measuring the TSCAP spectrum shows that the system is in configuration B. These conclusions are in agreement with the more complicated experiments reported in Ref. 2.

The photoionization rate versus energy was measured for each electronic emission process as follows. The M center was prepared in the desired configuration, A or B, with all traps filled. The desired charge state of the M center was then obtained by illuminating until saturation at a photon energy below the threshold for the electronic emission process of interest. All optically shallower states were thus emptied. The photoionization rate for the emission process of interest was then measured (as capacitance versus time) at increasing photon energies, one energy at a time. The initial configuration and charge state were reset before each measurement using the electrical and optical preparation steps just described. The photoionization rate was defined as the inverse of the time constant ($1/e$) of the exponential capacitance versus time trace. Using these procedures, one can examine a particular emission process independent of others until the emission rate of a higher threshold energy process becomes appreciable.

The results of measurements of photoionization rate

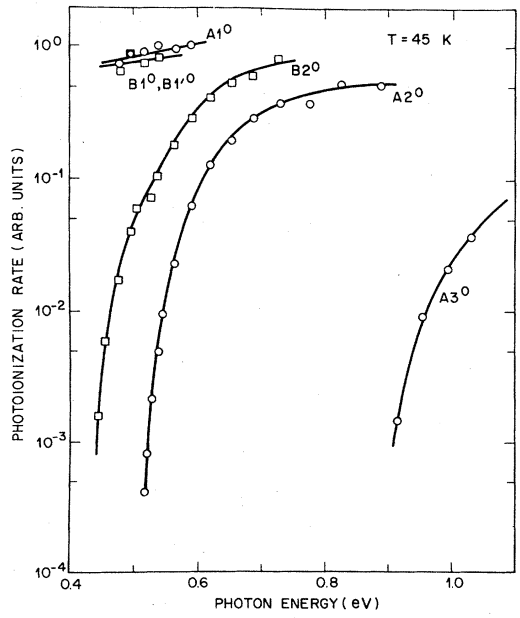

FIG. 4. Normalized photoionization rate specific to each M-center charge state versus photon energy. Open circles are for configuration-A transitions and open squares are for configuration-B transitions.

versus energy for the electron emissions of the M center are displayed in Fig. 4. These results are normalized to the incident illumination intensity. We do not report absolute values of the photoionization cross section because it is difficult to estimate an absolute value of the incident optical intensity for side-illuminated mesa diodes.

A commonly utilized procedure for determining optical transition energies involves fitting the photoionization spectrum over a wide range of photon energies (preferably at several temperatures) to a theoretical expression.[22,23] The Franck-Condon shift (defined in this context to be the difference between optical and thermally activated transition energies) is one of the parameters that is determined in the fitting procedure. Here, with data taken over limited energy ranges and at a single temperature, we take the transition energy to be the energy at the inflection point in the photoionization spectrum when plotted on a linear scale of photoionization rate versus energy.[24] From the data of Fig. 4 we determine the optical transition energies $E^0(A2)=0.68\pm0.1$ eV and $E^0(B2)=0.61\pm0.1$ eV. We set the following limits for the optical transition energies $E^0(A1)<0.4$, $E^0(B1,B1')<0.4$, and $E^0(A3)>1.1$ eV.

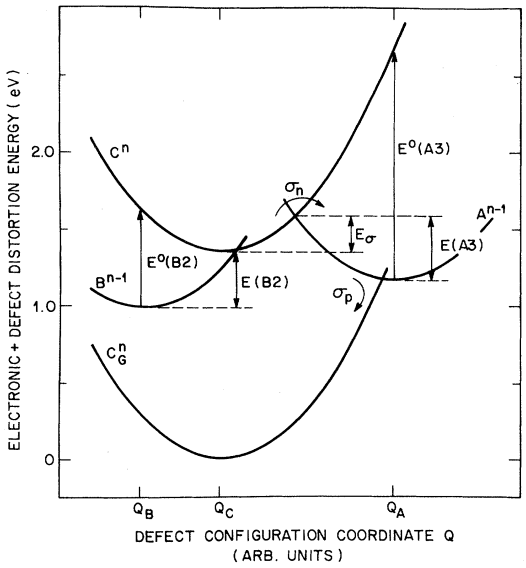

FIG. 5. CC diagram for the bistable characteristics of the M center.

IV. CONFIGURATION-COORDINATE DESCRIPTION

The data that have been presented show that the M center is indeed a complicated defect that is rich in phenomena. It is a multielectron trapping center; it is bistable, i.e., gives rise to spectra that correspond to two distinct configurations; it displays negative-U behavior (as will be discussed later) in configuration A, i.e., electron emissions $A2$ and $A3$ occur at the same temperature. On the basis of the spectroscopic data we have developed a CC description of the M center.

Our approach here will be to present those parts of the CC diagram that relate to the bistable and negative-U characteristics of the M center separately. On the basis of such diagrams the data presented in Secs. II and III will be discussed. Additional data on M-center transitions will be discussed at the end of this section.

A. M-center bistability

A simplified one-dimensional CC diagram that explains the bistable character of the M center is shown in Fig. 5. The curve labeled C_G^n corresponds to the total energy of the system in its ground state. The curve labeled C^n corresponds to the system energy for an unoccupied defect with a free-electron-hole pair present. (This curve is parallel to C_G^n and is increased in energy by the band gap.) The curves marked A^{n-1} and B^{n-1} correspond to the energy of the *two possible different configurations* of the M center when occupied by an electron with a free hole present. The superscripts correspond to the charge of the center.[25] We emphasize that curves A^{n-1} and B^{n-1} represent two different configurations *for the same charge state* of the M center. Charge state C^n can be accessed from both configurations and is thus common to both (C is for common).

Our discussion of the CC model will be classical throughout this work. Thus the thermal activation energy for a transition from a charge state corresponds to the energy difference between the crossing point of *initial-* and *final-state potential surfaces* and the *minimum* of the *potential surface* of the *initial charge state.* The energies of thermally activated transitions are shown with double-headed arrows, labeled as $E(P)$ where P is the label of the DLTS or TSCAP spectral emission feature.

An optical transition is vertical on a CC diagram with the transition energy given by the energy difference between *initial-* and *final-state potential surfaces* at constant Q. Optical transitions are shown as single-headed arrows with transition energies labeled as $E^0(P)$ where P again refers to the related TSCAP spectral feature.

The diagram shown in Fig. 5 is of the type proposed by Toyozawa for shallow-deep instability.[13,14] The M center has two configurations: one "ordinary" (B) and the other "self-trapped" (A), with the terms in quotations to be defined. When the M center is unoccupied with free carriers present, the equilibrium configuration of the system corresponds to $Q=Q_c$ on curve C^n. At this coordinate, the energy of B^{n-1} is less than that of C^n. Thus B^{n-1} is ordinary. In contrast to this ordinary state, the energy of A^{n-1} is much greater than that of C^n at $Q=Q_c$. The energy of A^{n-1} becomes less than that of C^n at the equilibrium configuration of the system when A^{n-1} is occupied, i.e., at $Q=Q_A$. A^{n-1} is said to be self-trapped because occupation of A^{n-1} brings this state into the band gap. E_σ represents a configurational barrier for capture into the self-trapped configuration A^{n-1}.

In this model of M-center bistability we focus on charge state A^{n-1} and emission $A3$ and omit other configuration-A charge states at this point for simplicity. From measurements of thermally activated emissions alone it is not clear that the anomalously large configurational relaxation occurs following $A3$, because $A2$ and $A3$ occur together. However, because these emissions

have different photoionization thresholds it is possible to determine unambiguously that following emission $A2$ the M center remains in configuration A, while following emission $A3$, it is found to be in configuration B as discussed in Sec. III.

The configuration and state of occupancy of the M center are determined in terms of the energetics shown in Fig. 5. At room temperature with reverse bias applied, all levels of the M center are unoccupied and the system is at $Q=Q_c$. If the diode is cooled with the bias on there are no electrons available for capture into states in the depleted region of the diode. At low temperature when the bias is removed to allow trap filling, only configuration B can be accessed because the barrier, E_σ in Fig. 5, cannot be surmounted. B^{n-1} is then filled.

If the diode is cooled with the bias off, free electrons are captured during the cooling procedure where E_σ can be surmounted. Since the electron emission $B2$ is faster than $A2$ and $A3$ (the TSCAP step is at lower temperature for $B2$ in Fig. 2), the occupation of configuration A is preferred at the outset of the cool down so that the defect becomes self-trapped into configuration A and the system is fixed at Q_A. The configuration which is obtained upon cooling and the relative stability of configurations A and B will be treated in more detail in Sec. IV B after we have discussed the negative-U ordering and binding energies of the energy levels in configuration A.

Each configuration described above provides a ladder of additional trapping levels that are ordinary. In configuration B these levels give rise to emissions $B1$ and $B1'$. In configuration A these levels give rise to emissions $A1$ and $A2$.[26] These ordinary trapping levels for configurations A and B could either be displayed on the same diagram or in additional CC diagrams with potential surfaces that would not involve self-trapping phenomena. (See Fig. 6 and further discussion Sec. IV B.)

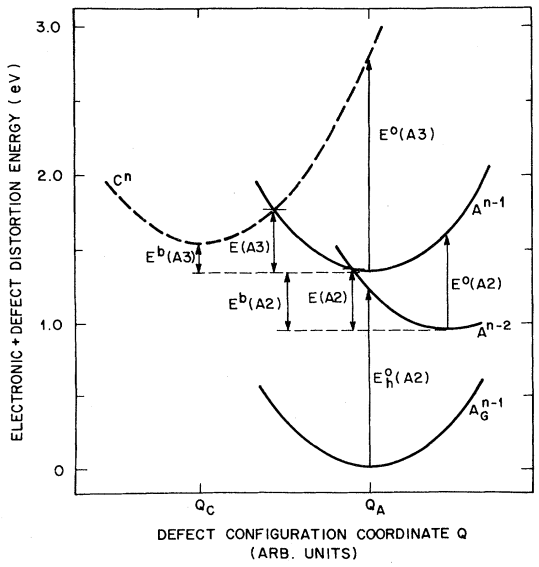

FIG. 6. CC diagram that displays the negative effective U of configuration-A levels.

The configurational transformation rates reviewed in Sec. II fit simply into the CC model. The rate $B\rightarrow A$, $k=10^7\exp(-0.24\text{ eV}/kT)$, corresponds to the thermally activated capture of an electron from the conduction band into A^{n-1} (activation energy E_σ in Fig. 5) as discussed above. The rate $k(A\rightarrow B)=10^{11}\exp(-0.42\text{ eV}/kT)$ corresponds to the thermally activated emissions $A2$ and $A3$. It should be noted that $A3$ could have a smaller emission activation energy than $E(A2)=0.42$ eV because emission $A3$ cannot occur until $A2$ has occurred. An estimate of the activation energy for $A3$ alone can be made from the observation that in curves 3 and 4 of Fig. 3(a), the $A3$ emission step does not move to lower temperature when $A2$ has already occurred. Thus if it is assumed (as we shall) that $A2$ and $A3$ have comparable emission rate prefactors then the activation energy $E(\text{A3})\simeq 0.42$ eV.

The measured optical and thermally activated transition energies allow B^{n-1} to be placed relative to C^n in the CC diagram shown in Fig. 5. A^{n-1} is placed on the basis of its thermally activated emission energy and the barrier for capture E_σ. The model, as constructed, shows that there should be an anomalously large Franck-Condon shift for emission $A3$ [The model predicts $E^0(A3)=1.48$ eV.] This is in accord with the optical data where $E^0(A3)>1.1$ while $E(A3)\approx 0.42$ eV. This large Franck-Condon shift is characteristic of the self-trapped nature of state A^{n-1} and is in marked contrast to state B^{n-1} which is characterized by an ordinary, small Franck-Condon shift.

While the configurational transformation $A\rightarrow B$ can be stimulated optically, there has been no optical process observed that leads to $B\rightarrow A$ transformation. This behavior is consistent with our CC model because the energy position of A^{n-1} at $Q=Q_c$ is well into the conduction band and, therefore, A^{n-1} cannot be filled by an optical transition from the valence band (that is, with photons of energy less than the band gap).

B. Negative-U ordering of M-center levels

In Sec. IV A the binding of an electron by a bistable charge state of the M center was considered. We discuss the multielectron trapping nature of configuration A in this section and the negative-U ordering of the energy levels. We also describe how the negative-U character of A leads to its increased stability with respect to configuration B.

The concept of negative electron-electron correlation energy or negative U was first introduced by Anderson.[27] If an ordinary center traps two electrons, it is expected that the second electron will be less tightly bound than the first by a positive energy U, due to the Coulomb repulsion between the trapped electrons. However, when the binding of the second electron leads to lattice relaxation, the effective electron-electron correlation energy is reduced and may even become negative for a sufficiently large, energy-lowering relaxation. When such a negative-U ordering of energy levels occurs the system is not stable in the singly occupied charge state for any position of the Fermi energy of the system. The silicon vacancy and the boron interstitial in silicon are examples of negative-U,

crystalline defect systems that have received recent attention.[8-12]

The TSCAP spectrum shown in Fig. 2(a) indicates that the M-center energy levels of configuration A may form a negative-U system. While the electron emission $A1$ occurs at the lowest temperature (ordinary ordering) the emissions $A2$ and $A3$ occur simultaneously (indicative of negative-U ordering).[8,10]

A CC diagram is shown in Fig. 6 for the trapping levels that give rise to emissions $A2$ and $A3$. We have omitted configuration-B curves for simplicity. The labeling of the configuration A states (with the free carriers necessary for charge balance) is as follows. Curve C^n in this diagram corresponds to the fully ionized M center with two free electrons and one free hole present. A^{n-1} corresponds to the singly occupied defect with a free-electron-hole pair present, A^{n-2} corresponds to the doubly occupied charge state with a free hole present, and A_G^{n-1} corresponds to a singly occupied defect with no free carriers present.

In Fig. 6, the charge state A^{n-1} is self-trapped as was discussed in Sec. IV A. Charge state A^{n-2}, however, is found to be ordinary from measurements of the thermally activated and optical transition energies $E(A2)=0.42$ eV and $E^0(A2)=0.68$ eV. It is on the basis of this data that A^{n-2} is placed on the CC diagram.

The most striking feature of the CC diagram shown in Fig. 6 is the difference between the Franck-Condon shifts for emissions from charge states A^{n-1} and A^{n-2}. As was discussed in Sec. IV A, the thermally activated emission energies for these charge states are roughly equal, i.e, $E(A3)\approx E(A2)=0.42$ eV. However, the photoionization transition energies differ by more than 0.5 eV. It is this difference in photoionization energies that has allowed us to examine the metastable charge state A^{n-1} independent of state A^{n-2}.

We remark that the activation energies determine the *kinetics* of electron emission. Negative-U behavior is, however, an *equilibrium* property of the system. Therefore, the equilibrium binding energies, $E^b(A3)$ *and* $E^b(A2)$, for the charge states A^{n-1} *and* A^{n-2}, respectively, are the relevant quantities in this context, rather than the emission activation energies. The binding energies shown in Fig. 6 correspond to the energy difference between equilibrium configurations of the occupied and unoccupied charge states of the defect. The binding energies $E^b(A3)=-0.18$ eV and $E^b(A2)=-0.40$ eV can be estimated from the CC model. The inverted ordering of these energies (an additional electron more tightly bound that its predecessor) is the defining characteristic of a negative-U system.

At this point it is appropriate to discuss the relative stabilities of configurations A and B. The equilibrium binding energy of state B^{n-1} is estimated to be -0.36 eV from our CC model. The binding energy of A^{n-1} is only -0.18 eV and is insufficient to make configuration A stable. If we consider only the trapping of this first electron, then it would appear that configuration B should be obtained if the sample were cooled sufficiently slowly with free electrons available. The system could be trapped kinetically in configuration A if cooled too quickly for equilibrium to be established because the emission activation energy of A^{n-1} is larger than that of B^{n-1}.

It is the inherently two-electron nature of the negative-U system that configuration A provides and not just a kinetic effect in the one-electron trapping system that leads to the occupation of configuration A upon cooling with the reverse bias off in our experiments. Because the levels of configuration A form a negative-U system, the binding energy of A^{n-2}, -0.40 eV, is greater than that of A^{n-1} and is sufficient to stabilize configuration A with respect to B. Thus, configuration A *is stable* and B is metastable.

C. Additional M-center features

In addition to the charge states described above that control the M-center configuration, there are the ordinary electron-emission features $B1$, $B1'$, and $A1$ that make each configuration of the M center observable in ordinary DLTS measurements. These emissions could, in principle, be included in the CC diagrams discussed above with additional levels that do not involve self-trapping.

Configuration B is more complicated than we have described to this point. From the DLTS spectrum in Fig. 1 we can see that configuration B consists of two different defects, not simply the multiple trapping levels of a single defect as in configuration A. The evidence for this is that the DLTS peak heights obey the relationship $B1+B1'=A1$. Because the DLTS peak $B2$ is asymmetric, it is also likely to be two unresolved peaks. A possible explanation of this behavior is that there is only one configuration for A^{n-1} but that there exist two structurally inequivalent configurations[1] for B^{n-1}—call these B^{n-1} and B'^{n-1}. If this example were correct then one should represent the $B^{n-1}-A^{n-1}$ and $B'^{n-1}-A^{n-1}$ systems by different CC diagrams. The splitting of configuration-B states introduces only minor perturbations to the transformation kinetics[1] and does not affect the essential physics of the electronic control of M-center configurations that we have described. However, this splitting may be providing a clue to the microscopic structural nature of the configurational metastability and should not be disregarded.

In previous work on the M center, the configurational transformation $A\rightarrow B$ was observed to occur upon hole injection.[1-3] In the CC model we have presented, this process corresponds to the capture of three holes by configuration A (which produces the same charge-state as the emission of three electrons). The capture of the third hole by the configuration-A system (the process labeled σ_p in Fig. 5) leads to rapid relaxation from Q_A to Q_C.

In addition to the optical transitions that promote electrons from filled defect levels to the conduction band, it is also possible to promote an electron from the valence band to an empty defect level. An example of such a transition is labeled $E_h^0(A2)$ in Fig. 6. We have observed no such transitions below a photon energy of 0.9 eV (the $A3$ photoionization threshold). Above 0.9 eV filling $[E_h^0(A2)]$ as well as emptying $[E^0(A3)]$ transitions were observed in parallel. The photoionization rate was observed to deviate strongly from exponential kinetics for level A^{n-1} with illumination at photon energies above 1.05 eV. This result limits our ability to measure the photoionization rate for A^{n-1} at higher energies.

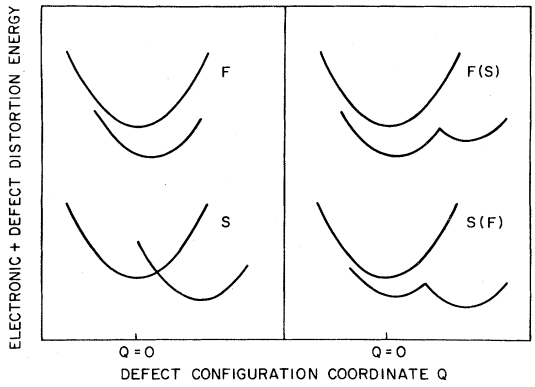

FIG. 7. Different classes of defect-level potential surfaces are shown for single-electron traps.

V. LARGE LATTICE RELAXATION AND THE *M* CENTER

The more familiar phenomena involving lattice relaxation for ordinary defects in semiconductors include capture by the multiphonon emission mechanism and the Franck-Condon shift observed between optical and thermally activated transition energies. In addition, several dramatic effects that involve very large lattice relaxation have been observed recently.[5,6] The *M* center is rich in such phenomena, displaying both extrinsic self-trapping and negative-*U* characteristics. In this section we discuss how the *M* center fits into the current theoretical and experimental picture of large lattice relaxation phenomena.

Toyozawa[13,14] has recently extended the concepts of self-trapping (i.e., of the polaron problem) to the case of extrinsic self-trapping of a carrier at a defect. The basic idea in Toyozawa's work is that the electron-phonon coupling strength increases as the orbital radius of the bound electron decreases. Thus the capture of a carrier tends to strengthen the potential that binds it, leading ultimately to self-trapping. Here we shall discuss our work in the context of his classification of defect potential surfaces. Figure 7 shows the features of the different classes of CC diagrams. The diagrams are labeled *F* (free) for what we have called ordinary defects and *S* for defects with self-trapping characteristics.[28] For defects of the *S* class there is an activation barrier for capture and there is no radiative capture process. Bistability can arise for some defects, in which case a charge state can have both *F* and *S* configurations with a barrier between the two. These cases are denoted $F(S)$ when the ordinary state is stable and the self-trapped state is metastable, and $S(F)$ for when the self-trapped state is stable and the ordinary state is metastable.

Examples have been reported in the literature which fall into the general classes of defects discussed by Toyozawa.[13,14] *DX* centers[7,18,29] are an example of defects of type *S*. Self-trapping in these centers gives rise to persistent photoconductivity at low temperatures. Cl in CdTe is another defect of the *S* type that displays persistent photoconductivity.[30] The model proposed to explain the photocapacitance quenching effect observed for EL2 is of the $F(S)$ type.[19] In the EL2 model there is an ordinary stable state and a self-trapped metastable state that can be obtained by optical excitation without a change of charge state at low temperatures. CdF:In provides an example of a center of $S(F)$ character.[6,20] For this center the self-trapped state is stable. Optical ionization of the center at lowered temperature populates the ordinary metastable state. As we have indicated each of these defect types has a different experimental manifestation of its self-trapping characteristics.

The *M* center, because of its multielectron trapping nature, is most intriguing and adds new features to those described above. If we consider just the A^{n-1} and B^{n-1} levels (Fig. 5) of the *M* center (i.e., consider a one-electron trapping system) our model is of the type $F(S)$ where the ordinary state would be most stable. However, the *M* center has a number of ordinary defect states associated with each configuration of its bistable charge state. Because of the large lattice relaxation associated with A^{n-1}, the ordering of energy levels in configuration *A* is inverted. The negative-effective-*U* ordering increases the stability of the self-trapped configuration. Thus, even though the multielectron trapping *M* center cannot be described properly by the classes of one-electron trap-potential surfaces shown in Fig. 7, we find that the self-trapped configuration *A* is stable and *B* is metastable so that the system effectively has $S(F)$ character. Toyozawa[13] has described generally this kind of behavior in multielectron systems. The *M* center is the first reported example of such a defect in a crystalline solid where self-trapping and negative effective *U* are intimately related.

VI. CONCLUDING REMARKS

The *M*-center model, as we have presented it, is based upon one-dimensional CC diagrams. This approximation should not be regarded as an inherent limitation. We realize, for instance, that B^{n-1} and A^{n-1} may involve lattice relaxations of a different nature and that a one-dimensional description is an oversimplification. Thus the representation of the defect system on a diagram with a single coordinate should only be regarded as being schematic. No part of our description precludes B^{n-1} from being represented along a different coordinate axis for instance.

In our CC models all the energy surfaces have been drawn with equal curvature, i.e., the spring constants are assumed not to depend on the charge state or configuration of the system. This approximation is used because there is insufficient data at present to determine the relative curvatures of the different energy curves. If $E^0(A3)$ could be determined (we have set a lower bound) or if the activation energies for capture were known for the various charge states, the curvatures of the energy surfaces could be adjusted to accommodate this data. Such modifications to the model would not change the qualitative nature of any of the energy surfaces or the picture of charge-state control of the defect configuration that we have described.

A more complete description of the *M* center will re-

quire structural information about the different configurations and the nature of the lattice relaxation. The only microscopic structural information available at present is the suggestion that the M center is a complex rather than a fundamental lattice defect because of its low introduction rate with room-temperature electron irradiation.[21] This idea is in keeping with the qualitative notion that metastable defects in covalent solids might often involve the structural rearrangement of a "defect molecule" as in molecular photochemistry. Large configurational relaxations are not restricted to complexes, however (the Si vacancy,[8–10,12] for example).

The CC model presented here is not simply a different conceptual way of expressing the electrostatic model[1] of the M center. Its explanation of the metastable behavior involves unique reaction pathways (in particular for the configurational change $B \rightarrow A$), and is independent of the specific driving force. Our photoionization data provide cross checks of the main features of the CC model.

We close by remarking that defects that display metastable and large-lattice-relaxation-related phenomena are more than a curiosity in covalent, semiconductor hosts. A growing number of examples of complicated, metastable centers in Si (Refs. 3 and 31), GaAs (Ref. 19), InP,[1–3] and in other III-V compounds[6] and alloys[7,18,29] exist. The M center has provided new insights into the nature of multielectron systems with self-trapping characteristics. As experimental methods for examining such centers and our theoretical understanding become refined, further intriguing examples of metastable defects should be discovered.

[1]M. Levinson, J. L. Benton, and L. C. Kimerling, Phys. Rev. B **27**, 6216 (1983).

[2]M. Levinson, M. Stavola, J. L. Benton, and L. C. Kimerling, Phys. Rev. B **28**, 5848 (1983).

[3]J. L. Benton and M. Levinson, in *Defects in Semiconductors II*, edited by S. Mahajan and J. W. Corbett (North-Holland, New York, 1983), p. 95.

[4]C. H. Henry and D. V. Lang, Phys. Rev. B **15**, 989 (1977). A good description of the application of CC diagrams to semiconductor defect problems is included in this work.

[5]C. H. Henry, in *Relaxation of Elementary Excitations*, edited by R. Kubo and E. Hanamura (Springer, New York, 1980), p. 19.

[6]J. M. Langer, in *New Developments in Semiconductor Physics*, Vol. 122 of *Lecture Notes in Physics*, edited by F. Beleznay, G. Ferenczi, and J. Giber (Springer, New York, 1980), p. 123.

[7]D. V. Lang and R. A. Logan, Phys. Rev. Lett. **39**, 635 (1977).

[8]G. A. Baraff, E. O. Kane, and M. Schlüter, Phys. Rev. Lett. **43**, 956 (1979).

[9]G. A. Baraff, E. O. Kane, and M. Schlüter, Phys. Rev. B **21**, 3563 (1980).

[10]G. D. Watkins and J. R. Troxell, Phys. Rev. Lett. **44**, 593 (1980).

[11]R. D. Harris, J. L. Newton, and G. D. Watkins, Phys. Rev. Lett. **48**, 1271 (1982).

[12]J. L. Newton, A. P. Chatterjee, R. D. Harris, and G. D. Watkins, Physica **116B**, 219 (1983).

[13]Y. Toyozawa, Physica **116B**, 7 (1983).

[14]Y. Toyozawa, Solid State Electron. **21**, 1313 (1978); Y. Toyozawa, in *Relaxation of Elementary Excitations*, edited by R. Kubo and E. Hanamura (Springer, New York, 1980), p. 3.

[15]D. V. Lang and L. C. Kimerling, Phys. Rev. Lett. **33**, 489 (1974).

[16]J. D. Weeks, J. C. Tully, and L. C. Kimerling, Phys. Rev. B **12**, 3286 (1975).

[17]L. C. Kimerling, Solid State Electron. **21**, 1391 (1978).

[18]D. V. Lang, R. A. Logan, and M. Jaros, Phys. Rev. B **19**, 1015 (1979); D. V. Lang, in *Deep Levels in Semiconductors*, edited by S. T. Pantelides (to be published).

[19]G. Vincent, D. Bois, and A. Chantre, J. Appl. Phys. **53**, 3643 (1982); G. Vincent and D. Bois, Solid State Commun. **27**, 431 (1978).

[20]U. Piekara, J. M. Langer, and B. Krukowska-Fulde, Solid State Commun. **23**, 583 (1977).

[21]M. Levinson, J. L. Benton, H. Temkin, and L. C. Kimerling, Appl. Phys. Lett. **40**, 990 (1982).

[22]M. Jaros, Phys. Rev. B **16**, 3694 (1977).

[23]A. Chantre, G. Vincent, and D. Bois, Phys. Rev. B **23**, 5335 (1981).

[24]A different treatment of our optical data could conceivably change the transition energies we have reported by the order of 0.1 eV. Such small changes would not affect the general features of the CC picture we present in any way. The error bars we report bracket the 10–90 % values of the photoionization edge.

[25]We measure only changes in charge state and can, therefore, only measure the relative charge state for a given defect. Thus the superscript n denotes the uncertainty in the charge of the unoccupied charge state.

[26]DLTS features do not appear for the emissions labeled $A2$, $A3$ in the TSCAP of Fig. 2 because the thermally activated capture of electrons by A^{n-1} is very slow in comparison to the duration of the "fill" pulse used in the DLTS measurement. At 175 K a filling time of 0.8 sec would be required.

[27]P. Anderson, Phys. Rev. Lett. **34**, 953 (1975).

[28]Toyozawa's notation (Refs. 13 and 14) is a holdover from the polaron problem. F is for free and S is for self-trapped.

[29]R. A. Craven and D. Finn, J. Appl. Phys. **50**, 6334 (1979).

[30]R. Legros, Y. Marfaing, and R. Triboulet, J. Phys. Chem. Solids **39**, 179 (1978).

[31]G. E. Jellison, J. Appl. Phys. **53**, 5715 (1982).